**Supplemental Information**

N*-quinoline-benzenesulfonamide

derivatives exert potent anti-lymphoma

effect by targeting NF-κB

Matko Kalac, Michael Mangone, Alison Rinderspacher, Shi-Xian Deng, Luigi Scotto, Michael Markson, Mukesh Bansal, Andrea Califano, Donald W. Landry, and Owen A. O'Connor

Supplemental Table 1. Halo Substituents at the 4- and 5-positions of the Thiophene Ring. Related to Figure 1.
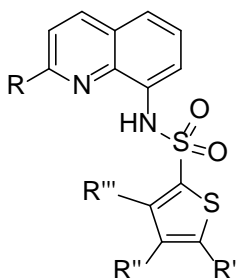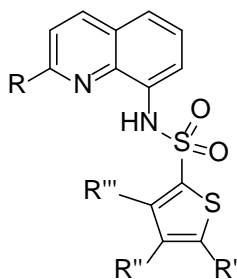

Compound #	R	R'	R"	R"'	Ly1 IC$_{50}$ [µM]	Ly10 IC$_{50}$ [µM]
O-4	CH$_3$	Br	H	H	1.4	1.5
O-19	H	Cl	H	H	0.8	0.7
O-25	CH$_3$	Cl	H	H	1.3	0.8
O-47	H	Cl	Cl	H	0.7	0.7
O-50	CH$_3$	Cl	Cl	H	>10	>10
O-49	H	Br	Br	H	1.4	1.5
O-52	CH$_3$	Br	Br	H	>10	>10
0-83	H	F	H	H	1.5	1.1

**Supplemental Table 2. Substituents at the 4- and 5-positions of the Thiophene Ring. Related to Figure 1.**
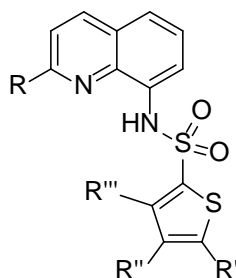
Compound #	R	R'	R"	R'''	Ly1 IC$_{50}$ [μM]	Ly10 IC$_{50}$ [μM]
O-48	H	Cl	NO$_2$	H	>10	>10
O-51	CH$_3$	Cl	NO$_2$	H	>10	>10
O-55	H	Cl	Br	H	0.5	0.5
O-56	CH$_3$	Cl	Br	H	>10	>10

Supplemental Table 3. Alkyl and Aryl Substituents at the 3-, 4-, and 5-positions of the Thiophene Ring. Related to Figure 1.
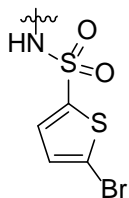

Compound #	R	R'	R"	R'''	Ly1 IC_{50} [µM]	Ly10 IC_{50} [µM]
O-61	H	Me	H	H	1.1	2.4
O-66	Me	Me	H	H	0.6	1.7
O-59	H	Et	H	H	1.4	2.6
O-64	Me	Et	H	H	1.6	3.2
O-60	H	H	H	Me	1.3	2.6
O-65	Me	H	H	Me	>10	>10
O-97	H	Ph	H	H	3.2	5.5
O-98	Me	Ph	H	H	4	27
O-87	H	H	CO_2H	H	>10	>10

Supplemental Table 4. Different Heterocyclic Substituents. Related to Figure 1.
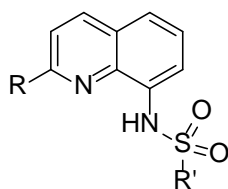
Compound #	R	R'	Ly1 IC$_{50}$ [µM]	Ly10 IC$_{50}$ [µM]
O-53	H		>10	>10
O-54	Me		6.3	5.4
O-90	H		>10	>10
O-57	H		1.7	3.1
O-58	Me		1.4	2.6
O-63	H		>10	>10
O-67	Me		Not tested	Not tested
O-62	H		>10	>10

Supplemental Table 5A. Different Cores. Related to Figure 1.

Compound #	CORE	Ly1 IC$_{50}$ [µM]	Ly10 IC$_{50}$ [µM]
O-84		>10	>10
O-85		6.3	5.4
O-88		>10	>10
O-89		1.7	3.1
O-91		1.4	2.6
O-94		>10	>10

Supplemental Table 5B. Different Cores.
Related to Figure 1.
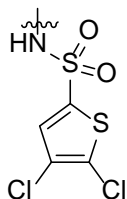
Compound #	CORE	Ly1 IC$_{50}$ [µM]	Ly10 IC$_{50}$ [µM]
O-92		>10	>10
O-93		>10	>10
O-103		>10	>10
O-111		NO DATA	5

Supplemental Table 6. Substituted Phenyl Groups. Related to Figure 1.
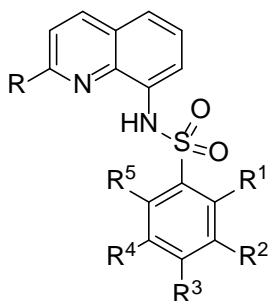
Compound #	R	R¹	R²	R³	R⁴	R⁵	Ly1 IC$_{50}$ [µM]	Ly10 IC$_{50}$ [µM]
O-68	H	Br	H	H	H	H	1.5	1.2
O-69	H	H	H	Cl	H	H	0.7	0.7
O-70	H	Cl	H	H	H	H	1.1	1.2
O-71	H	H	Cl	H	H	H	1.2	1.2
O-72	H	H	Br	H	H	H	1.9	1.5
O-73	H	F	H	H	H	H	0.9	1
O-74	H	H	F	H	H	H	0.7	0.7
O-75	H	H	H	F	H	H	0.7	0.7
O-76	Me	Br	H	H	H	H	3.7	3.9
O-77	Me	H	H	Cl	H	H	1.5	1.2
O-78	Me	Cl	H	H	H	H	3.8	3
O-79	Me	H	Cl	H	H	H	1.7	1.6
O-80	Me	H	Br	H	H	H	1.2	1
O-81	Me	F	H	H	H	H	1.8	1.9
O-82	Me	H	F	H	H	H	1.5	1
O-86	Me	H	H	F	H	H	2.1	2.3
O-95	H	H	H	Br	H	H	1	1.5
O-96	Me	H	H	Br	H	H	1.4	1.8
O-99	H	H	H	NO$_2$	H	H	>10	>10
O-104	H	H	OMe	OMe	H	H		>5
O-105	H	H	H	OMe	H	H		4.5
O-106	H	H	H	OCF$_3$	H	H		2.5
O-107	H	H	H	OCH$_2$CO$_2$H	H	H		>5
O-110	H	H	COOH	F	H	H	2	2
O-113	H	H	H	I	H	H		2

Supplemental Table 7. Substituted Cores. Related to Figure 1.
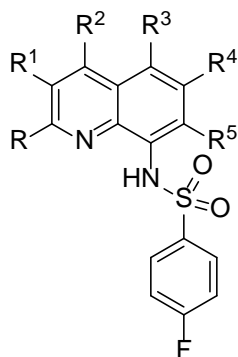
Compound #	R	R^1	R^2	R^3	R^4	R^5	Ly1 IC$_{50}$ [μM]	Ly10 IC$_{50}$ [μM]
O-109	H	H	Me	H	H	H	1.5	1.5
O-117	H	H	OMe	H	H	H	1.3	2.3
O-118	H	H	OCH$_2$CO$_2$H	OCF$_3$	H	H	>10	>10

Supplemental Table 8. Different Cores. Related to Figure 1.
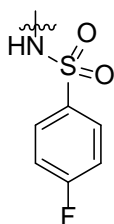
Compound #	CORE	Ly1 IC$_{50}$ [μM]	Ly10 IC$_{50}$ [μM]
O-102		>10	>10
O-108			>10
O-114		>10	>10
O-115		>10	>10

Supplemental Figure 1 – Spectral analysis of CU-O42, CU-O47, CU-O75 and CU-O102. Related to Figure 1B.

Spectral analysis - ^{1}H NMR and ^{13}C NMR spectra were recorded on an Agilent 400-MR 400-MHz NMR spectrometer. Chemical shifts are reported in parts per million using the residual proton or carbon signal ((CD3)2CO: δH 2.05, δc 29.84; CDCl3: δH 7.26, δc 77.16; and ((CD3)2SO: δH 2.50, δc 39.52) as an internal reference. The apparent multiplicity (s = singlet, d = doublet, t = triplet, q = quartet, m = multiplet) and coupling constants (in Hz) are reported in that order in the parentheses after the chemical shift. Liquid chromatography and mass spectrometry were performed on a Shimadzu 2020 UFLC mass spectrometer, using a Waters Sunfire column (C18, 5µm, 2.1 mm x 50 mm, a linear gradient from 5 % to 100 % B over 15 min, then 100 % B for 2 min (A = 0.1 % formic acid + H2O, B = 0.1 % formic acid + CH3CN), flow rate 0.2000 mL/min. High-resolution mass spectrometry was performed by Dr. Brandon Fowler at Columbia University.

CU-O42
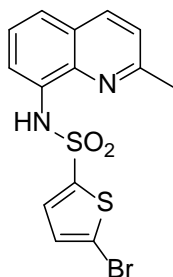
Yellow solid; Yield: 77 %; 1H NMR (400 MHz, (CDCl3): δ 9.34 (br s, 1H), 8.01 (d, *J* = 8.4 Hz, 1H), 7.83 (d, *J* = 7.6 Hz, 1H), 7.43 (d, *J* = 8.0 Hz, 1H), 7.35-7.30 (m, 3H), 6.88 (d, *J* = 3.6 Hz, 1H), 2.70 (s, 3H), ; 13C NMR (101 MHz, (CDCl3): δ 158.3, 140.8, 138.2, 136.5, 133.0, 132.7, 130.2, 126.5, 125.9, 123.2, 122.7, 120.2, 115.7, 25.3; LC-MS (M$^+$+H): 385.

CU-O47
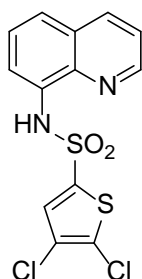
Yellow solid; Yield: 75 %; 1H NMR (400 MHz, (CDCl3): δ 9.33 (br s, 1H), 8.79 (d, *J* = 2.8 Hz, 1H), 8.17 (d, *J* = 8.0 Hz, 1H), 7.88 (d, *J* = 7.2 Hz, 1H), 7.59-7.51 (m, 2H), 7.48 (dd, *J* = 8.4 Hz, *J* = 4.4 Hz, 1H), 7.39 (s, 1H), ; 13C NMR (101 MHz, (CDCl3): δ 149.2, 138.8, 136.6, 133.0, 131.5, 128.5, 127.0, 124.8, 123.4, 122.4, 115.8; LC-MS (M$^+$+H): 359.

CU-O75
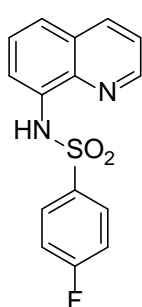
Clear, colorless crystals; Yield: 54 %; 1H NMR (400 MHz, (CD3)2CO): δ 9.40 (br s, 1H), 8.84 (dd, *J* = 4.4 Hz, *J* = 1.6 Hz, 1H), 8.34 (dd, *J* = 8.4 Hz, *J* = 1.2 Hz, 1H), 8.02 (dd, *J* = 8.8 Hz, *J* = 5.2 Hz, 2H), 7.87 (d, *J* = 7.6 Hz, 1H), 7.66 (d, *J* = 8.4 Hz, 1H), 7.60-7.53 (m, 2H), 7.23 (t, *J* = 8.8 Hz, 2H); 13C NMR (101 MHz, (CDCl3): δ 165.3 ($^1J_{C-F}$ = 255.5 Hz), 149.0, 138.7, 136.4, 135.5 ($^4J_{C-F}$ = 3.1 Hz), 133.7, 132.3, 132.2, 130.1 ($^3J_{C-F}$ = 9.9 Hz), 128.3, 126.9, 122.6, 122.2, 116.2 ($^2J_{C-F}$ = 22.8 Hz), 115.6; LC-MS (M$^+$+H): 303.

CU-O102
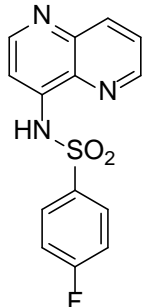
Orange-yellow solid; Yield: 44 %; 1H NMR (400 MHz, (CD3)2SO): δ 8.88 (d, *J* = 3.2 Hz, 1H), 8.46 (s br, 1H), 8.22 (d, *J* = 8.4 Hz, 1H), 8.04 (dd, *J* = 8.4 Hz, *J* = 5.2 Hz, 2H), 7.80 (dd, *J* = 8.8 Hz, *J* = 4.4 Hz, 1H), 7.43 (d, *J* = 6.8 Hz, 1H), 7.38 (t, *J* = 8.8 Hz, 2H); 13C NMR (101 MHz, (CD3)2SO): δ 164.0 ($^1J_{C-F}$ = 251.8 Hz), 149.0 (2C), 138.2, 136.2, 129.5 ($^3J_{C-F}$ = 9.1 Hz) (2C), 126.4 (2C), 116.1 ($^2J_{C-F}$ = 22.9 Hz)(2C), 107.8(2C); LC-MS (M$^+$+H): 304; ESI + HRMS (*m/z*): [M+H]$^+$ calcd. for C14H11FN3O2S: 304.0551, Found: 304.0556.

Supplemental Figure 2 – IC50 growth inhibition values in lymphoma cell lines (DLBCL and mantle cell lymphoma) as measured by ATP luminescence based assay after incubation with NQBS for 72h. Related to Figure 2A and 2B.
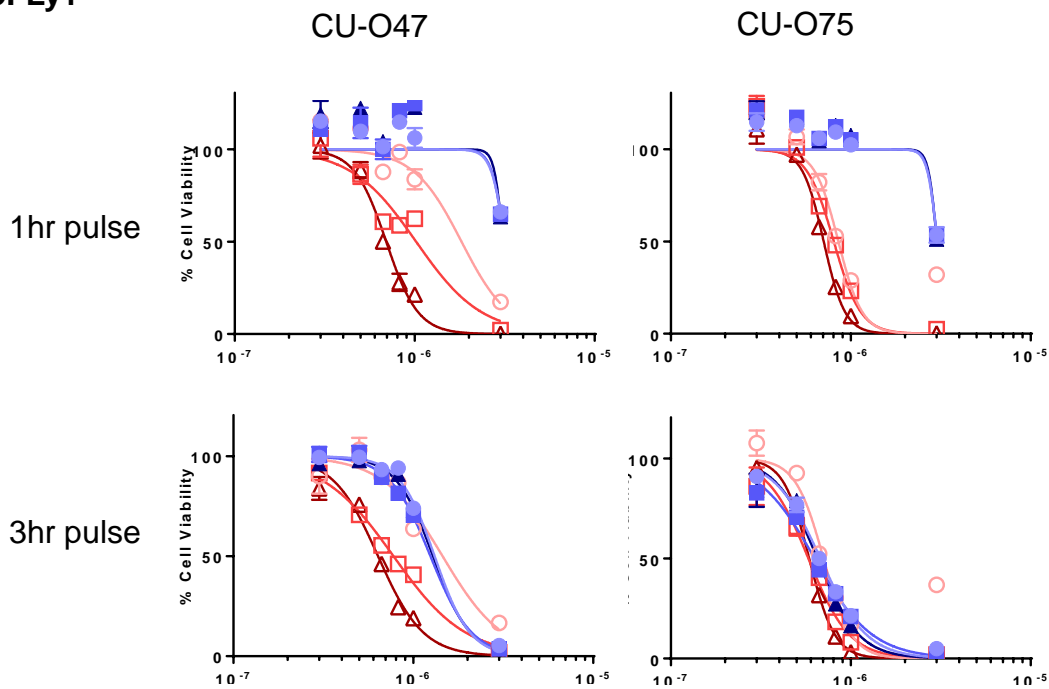
subtype	ABC DLBCL				GCB DLBCL		MCL
cell line	OCI-Ly10	SuDHL-2	HBL-1	RIVA	OCI-Ly1	SuDHL-6	HBL-2
IC_{50} (µM)	1.00	0.84	2.31	1.51	0.77	0.75	1.24

Supplemental Figure 3 – A pulse chase experiment analyzing cell growth inhibition in DLBCL cell lines treated with CU-O47 and CU-O-75. Related to Figure 2.
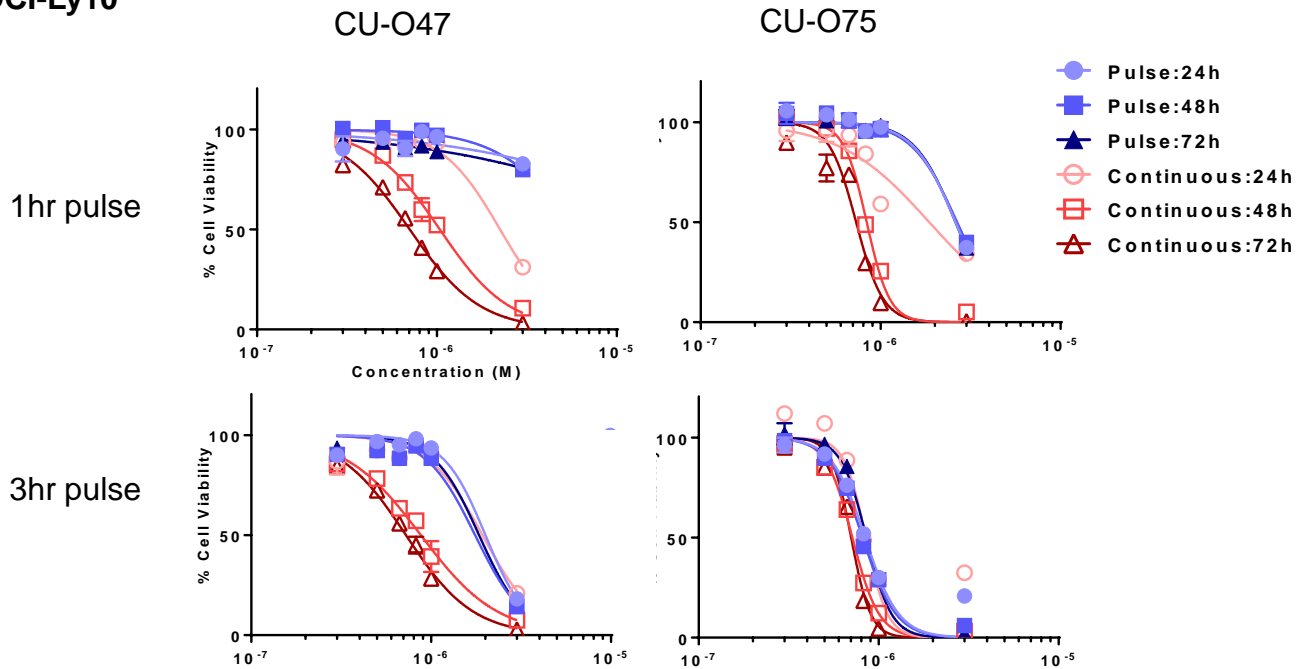
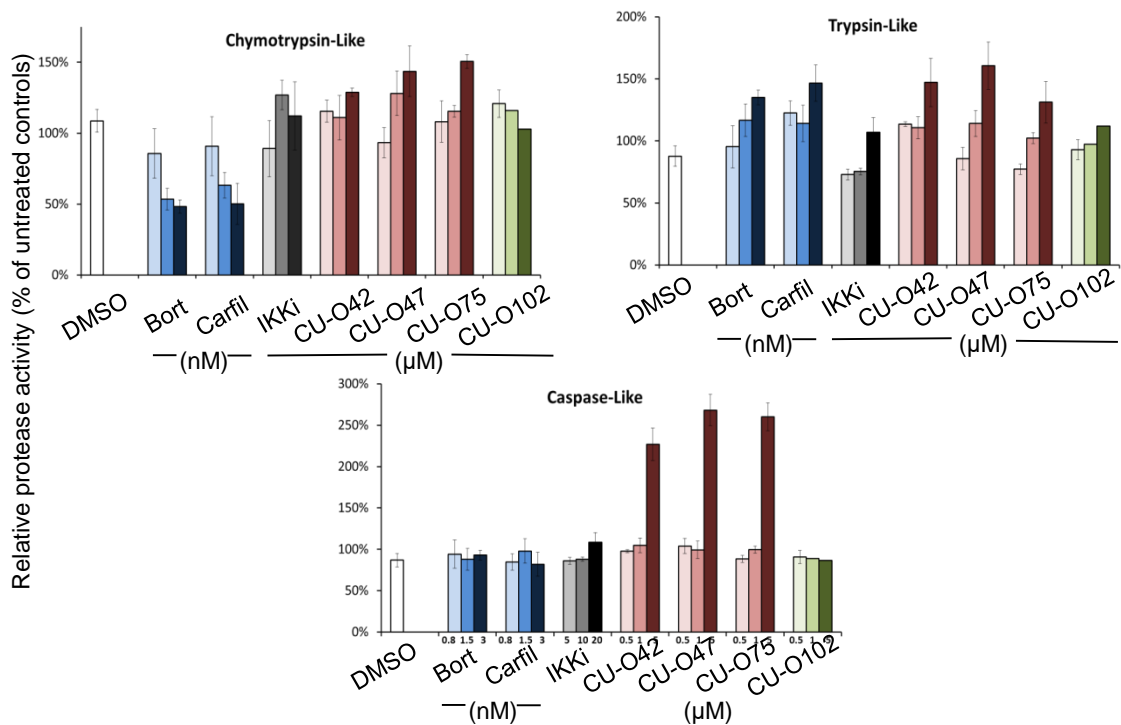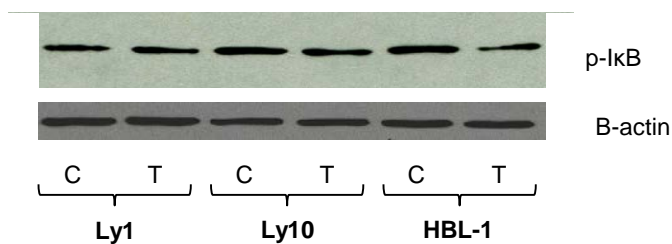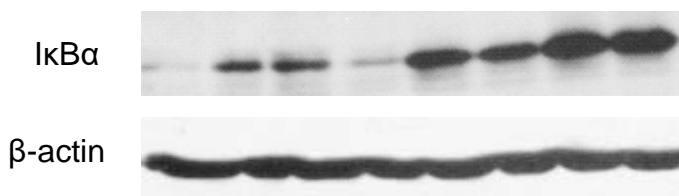**Supplemental Figure 4 – NQBS mechanism of action. Related to Figure 4.**

A.

B.

C = control
T = CU-O42 (4 µM)

C.

Supplemental Figure 5 – NQBS pharmacokinetics and toxicity. Related to Figure 6.

A.

Route
◆ Intraperitoneal
○ Oral

100 mg/kg of single dose CU-O75

Cumulative AUC

Time	IP	PO
0.5	834	127
2	4094	648
6	6489	1221
24	8215	2247

IC$_{50}$

y-axis left: CU-O75 (ng/ml)
y-axis right: CU-O75 (uM)
x-axis: Time (hrs)

B.

weight

y-axis: weight (mg)

— 10mg/kg
— 1mg/kg
— 0.1mg/kg
— control

x-axis: day 1, day 4, day 8

C.

WBC with differential

■ Eo
■ Mo
■ Ly
■ Neu

x-axis: normal, DMSO, 10mg/kg, 25mg/kg

RBC

x10^{6}/mm

x-axis: normal, DMSO, 10mg/kg, 25mg/kg
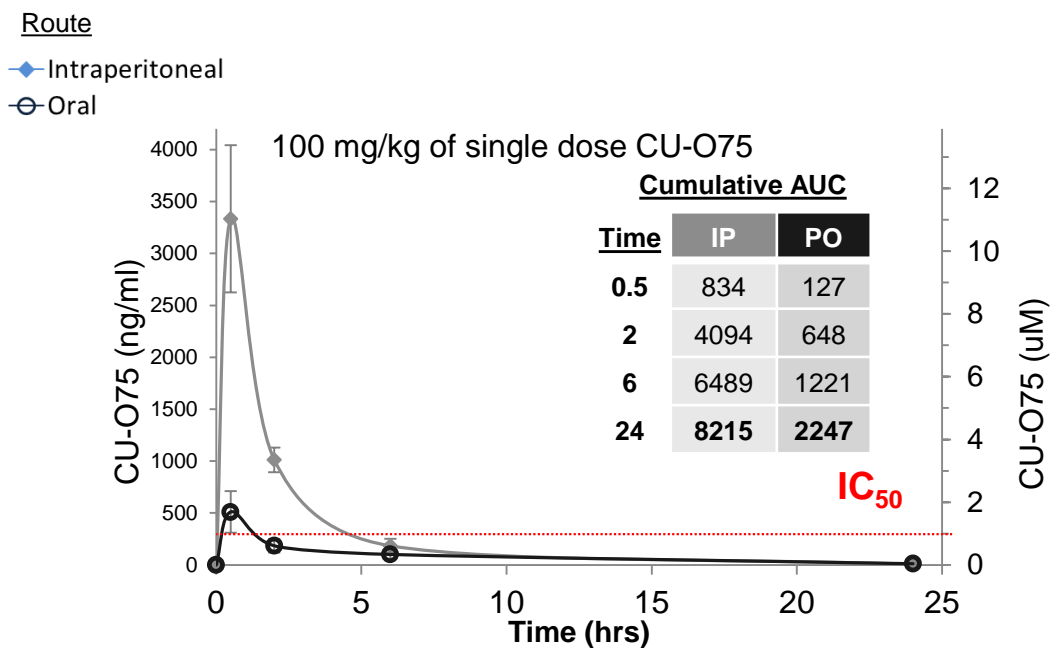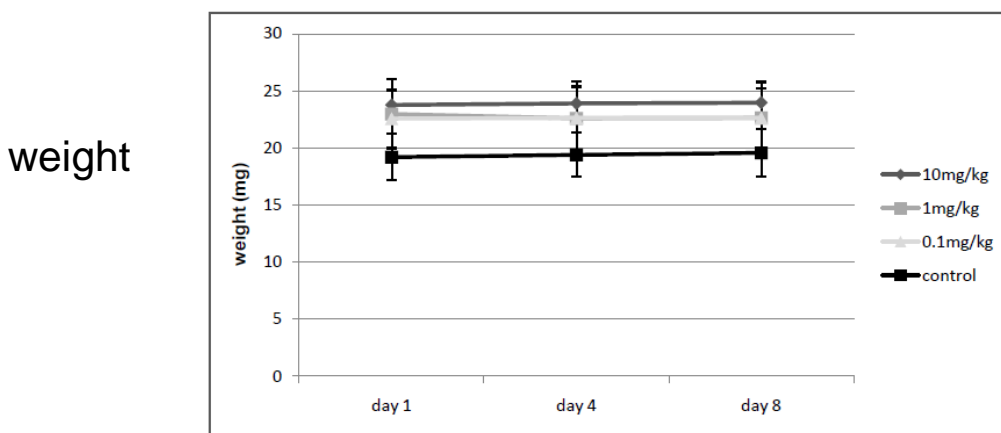
Transparent Methods

Cell lines. OCI-Ly1, OCI-Ly7 and Su-DHL6 are germinal center diffuse large B-cell lymphoma cell lines; OCI-Ly10, OCI-Ly3, RIVA, Su-DHL8 and Su-DHL2 are activated B-cell DLBCL lines; HBL-2 is a mantle cell lymphoma line. All the cell lines with the exception of Su-DHL6 were grown in IMDM medium with 10% fetal calf se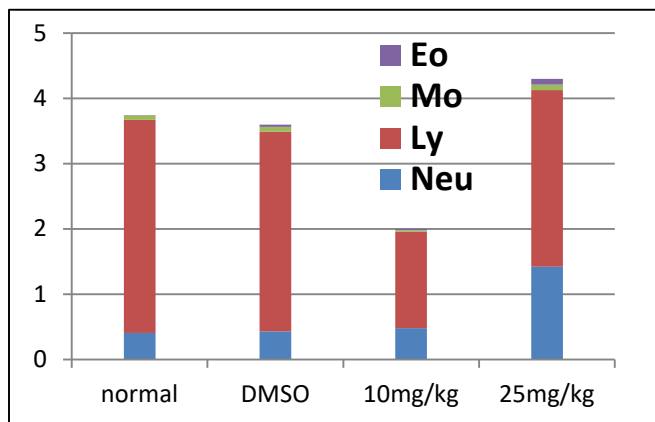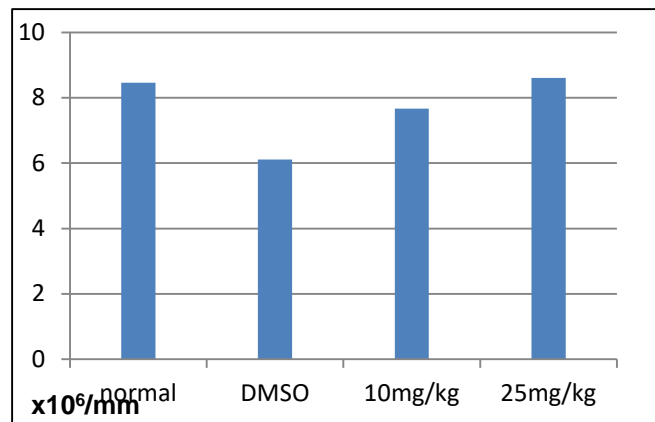rum (FCS); Su-DHL6 was grown in RPMI medium with 10% FCS. Fresh medium was added every 2-3 days and the cells were kept at a cell concentration of $0.3\text{-}0.8 \times 10^6$/mL. Cell lines were kindly provided from Dr. Ricardo Dalla Favera's lab and German Collection of Microorganisms and Cell Cultures GmbH and were verified by the ATCC.

Materials including cell growing medium and fetal calf serum were purchased from Thermo Fisher.

Compound synthesis.

General Procedure

Conditions A: 8-Aminoquinoline (1 equiv) was stirred in a 2:1 mixture of methylene chloride and pyridine at room temperature. The respective sulfonyl chloride (1 equiv) was added. The reaction mixture was stirred overnight, then concentrated *in vacuo* and purified via column chromatography (1:1 hexanes:ethyl acetate).

Conditions B: The respective sulfonyl chloride (1 equiv) was stirred in methylene chloride at room temperature. 8-Aminoquinoline (1 equiv) was added, followed by triethylamine (3 equiv). The reaction mixture was stirred overnight, then concentrated *in vacuo* and purified via column chromatography (1:1 EtOAc:CHCl$_3$).

Cell viability was evaluated using the Cell-Titer-Glo Reagent (Promega) as previously reported (Kalac et al., 2011). Cells were counted and re-suspended at an approximate concentration of 3×10^5 per well in a 96-well plate and incubated at 37°C in a 5% CO$_2$ humidified incubator for up

to 72 hours. Subsequently, NQBS were added at concentrations from 100 nmol/L up to 20 µmol/L to determine growth inhibition curves for all cell lines. Following incubation at 37°C in a 5% CO_2 humidified incubator, 100µL from each well was transferred to a 96-well opaque-walled plate; CellTiter-Glo reagent was used according to the manufacturer's instruction. The plates were allowed to incubate at room temperature for 10 minutes before recording luminescence with a Synergy HT Multi-Detection Microplate Reader (Biotek Instruments, Inc.). Each experiment was done in triplicate and repeated at least twice.

<u>Flow cytometry.</u> To study apoptosis, Yo-Pro-1 and propidium iodide (PI) were used (Vybrant apoptosis assay kit 4, Invitrogen, Carlsbad, CA) as previously described[1]. Briefly, cells were seeded at a density of 3×10^5/mL and incubated with NQBS for up to 72 hours. A minimum of 1×10^5 events were acquired from each sample. To quantitate apoptosis, Yo-Pro-1 and propidium iodide (PI) were used (Vybrant apoptosis assay kit #4, Invitrogen) according to the manufacturer's instruction. The fluorescence signals acquired by a FACSCalibur System were resolved by detection in the conventional FL1 and FL3 channels. Cells were considered early apoptotic if Yo-Pro-1 positive but PI negative, late apoptotic if Yo-Pro-1 and PI positive, and dead if only PI positive. Each experiment was done in triplicate and repeated at least twice.

<u>Western blotting</u> was performed as previously reported[1]. Briefly, cells were incubated with the same concentrations of NQBS used in the apoptosis and caspase assays under normal growth conditions for up to 24 hours. Proteins from total cell lysates were resolved on 4% to 20% SDS-PAGE and transferred onto nylon membranes. Membranes were blocked in PBS, 0.05% Tween 20 containing 5% skim milk powder or BSA and were then probed overnight with specific primary antibodies. Antibodies were detected with the corresponding horseradish peroxidase–linked secondary antibodies. Blots were developed using SuperSignal West Pico chemiluminescent substrate detection reagents. The membranes were exposed to X-ray films for various time intervals. The images were captured with a GS-800 calibrated densitometer (Bio-Rad).

Antibodies were purchased from the following vendors:

1. Cell Signaling: p50 (#3035), p65 (#8242), Ku-80 (#2753), Caspase 8 (#4790), PARP (#9532), Lamin B1 (#13435), XIAP (#14334), BID (#2002), beta actin (#3700), pan ubiquitin (#3936), anti-rabbit (#7074) and anti-mouse (#7076);

2. Santa Cruz: IκBα (sc-373893).

Nuclear protein extracts were prepared using the NE-PER Nuclear and Cytoplasmic Extraction Reagents (Thermo Fisher) as per manufacturer's instructions.

Immunoflorescence was performed as follows. After incubation with NQBS for 1-12 hours, the samples were placed on the slides using the cytospin. After fixation in 10% formalin and 100% methanol, the slides were transferred to the blocking buffer (10% nonfat dry milk) and incubated with primary antibody in the humidity chamber overnight. The slides were then incubated with fluorochrome-conjugated secondary antibody for 45 minutes and mounted with 4,6-diamidino-2-phenylindole. The images were collected using Nikon Eclipse TE 2000-E inverted epifluorescent microscope, a 40×/0.60 oil objective, and a Nikon Photometrics Coolsnap HQ2 camera. The images were analyzed using NIS-Elements AR 3.2 software and Volocity 5.5.1 software. Anti-p50 (#3035), anti-Ku80 (#2753) antibodies from Cell Signaling and Cy2- and Cy3-conjugated donkey anti–rabbit IgG (Jackson ImmunoResearch) secondary antibody were used. DAPI staining was used for nuclear localization (ThermoFisher).

Electrophoretic mobility shift assay (LightShift® Chemiluminescent EMSA Kit) was purchased from Thermo Fisher and performed as per manufacturer's instructions. Cells were incubated in the same manner as for immunoblotting. Cell pellets were collected after incubation with NQBS for 3-24h. Nuclear protein extracts were prepared using the NE-PER Nuclear and Cytoplasmic Extraction Reagents (Thermo Fisher) as per manufacturer's instructions. Collected samples and controls were run on a polyacrylamide gel in 0.5X TBE and transferred onto nylon membranes.

Membranes were subsequently cross-linked at 120mJ/cm2 using a commercial UV-light crosslinking instrument equipped with 254nm bulbs for 60 seconds. Membranes were then incubated in blocking buffer, washed and incubated in Substrate Equilibration Buffer and Substrate Working solution. The membranes were exposed to X-ray films for various time intervals. The images were captured with a GS-800 calibrated densitometer (Bio-Rad).

Kinome screen. We utilized KINOMEscan platform as per manufacturer's instructions (DiscoverX, Fremont, CA).

Internal Coordinate Mechanics (ICM) software was utilized as previously reported (Neves et al., 2012). We have used the following p50-p65-IκBα structure: https://www.rcsb.org/structure/1IKN

ICM software can be downloaded from: https://www.molsoft.com/download.html

Cellular thermal shift assay as previously described (Jafari et al., 2014). OCI-Ly10 cells were seeded at 4 x 10^5/mL and incubated with NQBS for 3h. The cells were subsequently washed and re-suspended in warmed PBS and protease inhibitor at a concentration of 3 x 10^7/mL. An aliquot (100μL) was transferred to PCR tubes which were placed on a thermocycler. Samples were heated at temperatures from 40-55 ⁰C at the gradient program (3 minutes heated gradient, 3 minutes 25 ⁰C). Samples were snap frozen and places in -80 ⁰C overnight. This was followed by cell lysis and the separation of cell debris and aggregates from the soluble protein fraction. Immunoblotting was used to analyze the results.

Generation of Gene Expression Profiles and DeMAND analysis was performed as previously described (Wee et al., 2015). We have used OCI-Ly10 samples treated with DMSO; IC20 value of CU-O75; and 1/10 of the IC20 value of CU-O75 at 12 and 24h. Download of DeMAND software available at: http://califano.c2b2.columbia.edu/demand

GSEA was performed as previously described (Subramanian et al., 2005). OCI-Ly10 samples used for GSEA were treated with DMSO; IC20 value of CU-O75; and 1/10 of the IC20 value of CU-O75 at 12 and 24h

In vivo studies. Mouse xenograft models were previously described[1]. Briefly, 10^{10} HBL-1 and OCI-Ly1 cell lines were injected subcutaneously to flanks of 4-6-week-old SCID beige mice (n=10 per group). Once the tumors were visually observed, they were measured and when they approached 55 mm^3, mice were randomized into treatment groups, either DMSO control or the NQBS treated ones. Volumes were measured every 3 days. Mice were sacrificed if tumor volumes exceeded 2000 mm^3. This study was undertaken in accordance to Columbia University's IUCAC approved protocol.

We also used genetically engineered transgenic mouse (n=3) using a CherryLuciferase fusion gene targeted to the CD19 locus to achieve B-cell–restricted fluorescent bioluminescent emission in transgenic mouse models of living mice as previously described[Error! Bookmark not defined.]. This study was undertaken in accordance to New York University's IUCAC approved protocol.

Statistics. IC50 (half the maximal inhibitory concentration) for each cell line was calculated using the Calcusyn Version 2.0 software (Biosoft, Cambridge, UK). The Wilcoxon rank-sum test was used to calculate the statistical significance *in vivo* for both actual and relative tumor volume. Relative tumor volume was calculated by comparing the actual volumes divided by the volumes on day 1 between the groups. A global test for significance was conducted by calculating the area under the actual (or relative) tumor volume curves using the trapezoidal rule.

Supplemental References

Jafari R, Almqvist H, Axelsson H et al. The cellular thermal shift assay for evaluating drug target interactions in cells. Nat Protoc. 2014;9:2100-22.

Kalac M, Scotto L, Marchi E et al. HDAC inhibitors and decitabine are highly synergistic and associated with unique gene expression and epigenetic profiles in models of DLBCL. Blood. 2011; 118:5506-16.

Neves MAC, Trotov M, Abagyan R. Docking and scoring with ICM: the benchmarking results and strategies for improvement. J Comput Aided Mol Des 2012; 26:675–86.

Subramanian A, Tamayo P, Mootha VK et al. Gene set enrichment analysis: A knowledge-based approach for interpreting genome-wide expression profiles. PNAS. 2005;102:15545-50.

Woo Hoon J, Shimoni Y, Yang WS et al. Elucidating Compound Mechanism of Action by Network Perturbation Analysis. Cell. 2015;162: 441–51.